

32 **Summary**

33 **The low G+C Gram positive bacteria represent some of the most medically and industrially**
34 **important microorganisms. They are relied on for the production of food and dietary**
35 **supplements, enzymes and antibiotics, as well as being responsible for the majority of**
36 **nosocomial infections and serving as a reservoir for antibiotic resistance. Control of gene**
37 **expression in this group is more highly studied than in any bacteria other than the Gram**
38 **negative model *Escherichia coli*, yet until recently no structural information on RNA**
39 **polymerase (RNAP) from this group was available. This review will summarise recent reports**
40 **on the high resolution structure of RNAP from the model low G+C representative *Bacillus***
41 ***subtilis*, including the role of auxiliary subunits δ and ϵ , and outline approaches for the**
42 **development of antimicrobials to target RNAP from this group.**

43

44

45

46

47 **Introduction**

48

49 RNAP structures from multiple bacterial species have been determined. Within molecular
50 microbiology, two organisms have dominated research into transcription and its regulation.
51 *Escherichia coli*, a Gram-negative bacterium, has been extensively studied to understand fundamental
52 mechanistic aspects of transcription and its regulation *e.g.* (1). *Bacillus subtilis*, a Gram-positive
53 organism, has been extensively studied for the regulatory processes associated with the initiation of
54 differential gene expression followed by compartment-specific transcription activation and gene
55 expression during the developmental process of sporulation (2).

56

57 At a structural level, RNAP from *E. coli* (RNAP_{EC}) has been studied for many years and with the
58 advent of modern cryo electron microscopy and single particle analysis techniques (cryoEM)(3), was
59 one of the first pseudo-atomic resolution multi-subunit RNAP structures solved (4). Prior to the
60 advent of these current resources, high resolution structural data from X-ray crystallography was
61 largely obtained from thermophiles for which little molecular biology data on transcription and its
62 regulation had been performed. Knowing the structure of RNAP_{EC} allowed the reconciliation of
63 structural and functional data in one system which has enabled profound new insights into the
64 mechanisms of transcription and its regulation *e.g.* (5,6)(7,8).

65

66 Such structural data on the Gram-positive *B. subtilis* system has been lagging, but high resolution
67 structures of several important complexes of *B. subtilis* RNAP (RNAP_{BS}) have been recently
68 published that enable a similar reconciliation of structural and molecular data (9-11). Despite the
69 considerable similarity between all multi-subunit RNAPs from bacteria, there are important
70 mechanistic differences that can now be examined. For example, initiation complexes tend to undergo
71 multiple rounds of abortive initiation prior to leaving the promoter region and entering the elongation
72 phase in *E. coli*, but similar effects are not observed in *B. subtilis* (12,13). The concentration and
73 identity of the initiating NTP ([iNTP]) also has a major effect on transcription efficiency in *B. subtilis*
74 (14).

75

76 Increasing our understanding of transcription regulation through structure-function studies is
77 particularly important as *B. subtilis* is an industrially significant organism used in the production of
78 enzymes (proteases, lipases, amylases), surfactants, and antibiotics (bacitracin) which have highly
79 complex regulatory circuits controlling the expression of their genes. As a member of the *Firmicutes*,
80 it is closely related to many of the most important clinical pathogens such as *Staphylococcus*,
81 *Streptococcus*, *Enterococcus*, and *Clostridia*. In this review we will examine the structure of RNAP_{BS}
82 and compare it with that of other bacteria, focussing on its unique features and auxiliary subunits and
83 include reference to homologous RNAPs from closely related *Firmicutes* pathogens and how this
84 information could be exploited in structure-based drug design.

85

86

87 ***Overall structure: RNA polymerases from the low G+C Firmicutes.***

88

89 All bacterial RNAPs have a similar overall subunit composition comprising two α subunits that form
90 an asymmetric dimer scaffold upon which the catalytic β and β' subunits assemble (Fig. 1). Due to
91 the lack of lineage-specific inserts (see below) RNAP_{BS} is more compact (shorter and narrower) than
92 other bacterial RNAPs: 150 Å \times 112 Å \times 123 Å (L \times W \times H), vs 157 \times 153 \times 136 Å; *E. coli*, 183 \times
93 107 \times 115 Å; *Mycobacterium smegmatis*, and 170.1 \times 110.1 \times 127.8 Å; *Thermus thermophilus* (10).

94

95 Transcription initiation involves the RNAP holoenzyme, promoter DNA, and transcription factors
96 (TFs). The primary housekeeping σ transcription factor in *Bacillus subtilis*, σ^A , contains sub-domains
97 $\sigma_{1.1}$, σ_2 , $\sigma_{3.1}$, $\sigma_{3.2}$, and σ_4 . The holoenzyme structure (core + σ^A) shown in Fig. 1A is based on the
98 complex with multidrug resistance regulator BmrR (9) and shows an open complex (DNA strands
99 separated at the -10 region, red oval, and template strand inserted in the active site within the primary
100 channel). In this structure much of the lineage-specific β ln5 insertion (see below) is missing, but the

101 flexible β -flap tip, important in binding essential transcription factor NusA (15), is visible and binds
102 to the σ_4 domain that also binds the -35 promoter sequence (red circle, Fig. 1A). In combination with
103 the transcription elongation complex (EC) (10), a near complete structure of the *B. subtilis* enzyme
104 can be modelled. The location of the primary (DNA binding) and secondary (NTP entry) channels
105 are marked as dashed circles in the EC and shown in Fig. 2B. It should be noted that the α -C terminal
106 domain that interacts with both transcription factors and DNA sequences was absent in all RNAP_{BS}
107 structures reported to date, due to the highly flexible sequence connecting the N- and C-terminal
108 domains, and lack of DNA/transcription factor for the α -C terminal domain to bind to. The structure
109 of this important DNA and protein interaction domain has been solved in complex with the
110 transcription factor Spx (16) enabling inclusion in models based on transcription initiation or
111 antitermination complex structures from other organisms (17,18) making it possible to further
112 augment the structures presented here.

113

114 A small, highly conserved, ω subunit binds around the C-terminus of the β' subunit and is associated
115 with enhancing subunit folding and incorporation of the β' subunit into the core structure (19,20). The
116 *Bacilli* and *Lactobacilli*, but not *Clostridia*, also possess an additional small subunit named ε ,
117 previously annotated as a second ω subunit (dark green, Fig. 1A and B), who's function has proven
118 to be enigmatic (21-23). Determination of the X-ray crystal structure of ε revealed it showed
119 remarkable similarity to the *E. coli* phage T7 gp2 that binds the β' jaw region of RNAP (labelled in
120 Fig. 1D) where it inhibits transcription initiation by the host cell RNAP (21,24). Based on this
121 similarity, it was hypothesised that ε could be involved in phage protection through binding to the β'
122 jaw of RNAP_{BS} (21,23). Determination of the structure of *B. subtilis* holoenzyme and a transcription
123 recycling complex comprising core RNAP with the ATP-dependent remodelling factor Held
124 revealed ε bound in a pocket formed mainly by the β' and α_1 subunits behind the secondary channel
125 on the downstream side of the enzyme (Fig. 1B; (9-11). The location of ε overlaps that of the β ln10
126 and -12 inserts of *Thermus thermophilus* RNAP as well as a region of Archaeal/Eukaryotic Pol II
127 Rpo3/RPB3 associated with enzyme stability, suggesting a similar role for ε in organisms, such as *B.*
128 *subtilis*, that are meso-thermophilic and capable of vigorous growth up to \sim 53 °C (10).

129

130 Major functional motifs in the β and β' subunits common to other bacterial RNAPs that are important
131 in DNA strand separation and rewinding (β fork loop, β' -rudder, -lid, -zipper) DNA clamping (β -
132 protrusion, -gate loop, β' clamp helices, N-terminal β' clamp), DNA binding cleft flexibility (β switch
133 3) *etc* are all highly conserved in the *B. subtilis* enzyme and are labelled in Fig. 1C and D (10,11).
134 However, given the differences in aspects of transcription such as open complex stability (above)
135 between *B. subtilis* and *E. coli*, sequence differences and/or insertions (e.g. the β' S13 insertion into

136 the trigger-loop in *E. coli*), these regions remain important areas of focus in structure-function studies
137 in the *Firmicutes*.

138

139 Across the eubacteria the β and β' subunits contain lineage-specific inserts that are largely of unknown
140 function (25,26). Despite the role of most of these lineage-specific inserts being unknown, the β ln9
141 insert in the β subunit of *E. coli* RNAP has recently been putatively implicated in coupling
142 transcription and translation under certain conditions (27). Elucidation of the structure of RNAP_{BS}
143 revealed the structure of the only major lineage-specific insert in *Firmicutes* RNAPs (labelled β ln5
144 in Fig. 1C) (10). Reconciliation of data from previous studies indicates that the β ln5 insert is involved
145 in binding to the C-terminal tudor domain of helicase/translocase PcrA (28,29) that is known to
146 interact strongly with RNAP (28,30-32). The β ln5 insert is located within the major lobe of the β
147 subunit which is one of the least highly conserved regions in bacterial RNAPs and is the site of many
148 other lineage-specific inserts (25,26) raising the possibility this part of RNAP may be important in
149 providing a platform for lineage-specific transcription factor interaction modules. Overall, due to the
150 lack of lineage-specific inserts (excepting β ln5), RNAP from *B. subtilis* and other low G+C Gram
151 positive bacteria represent the smallest multi-subunit RNAPs: *B. subtilis* $\alpha_2\beta\beta'\omega\epsilon$, 352.32 kDa;
152 *Mycobacterium tuberculosis* $\alpha_2\beta\beta'\omega$, 363.19 kDa; cf. *E. coli* $\alpha_2\beta\beta'\omega$, 389.05 kDa.

153

154 ***The δ subunit***

155

156 Many *Firmicutes* also contain a small δ subunit that is tightly associated with and present at
157 approximately equimolar concentrations with respect to RNAP (30,33). δ is a bipartite protein of 173
158 amino acids with a globular N-terminal domain and unstructured highly acidic C-terminal domain of
159 approximately equal sizes (34,35). It has been implicated in multiple regulatory roles associated with
160 transcription initiation, inhibition of non-specific transcription, transcription complex recycling and
161 transcription termination (23,36-41). The binding site of δ on RNAP has been the subject of
162 considerable speculation. Independent studies placed it adjacent to the RNA exit channel (42) or close
163 to/inside the DNA binding cleft (43). Determination of the structure of a *B. subtilis* RNAP-Held- δ
164 recycling complex by (11) showed δ binds on the β' subunit close to the DNA binding cleft, consistent
165 with findings of *in vivo* cross-linking mass spectrometry studies (43), reconciling the observed
166 biochemical effects of δ on transcription with the structure of a δ -containing transcription complex.
167 In subcellular localisation studies of δ and RNAP in dual fluorescent protein labelled cells, δ perfectly
168 colocalised with RNAP and was present at similar levels suggesting it is associated with RNAP
169 throughout all stages (initiation, elongation, termination) of the transcription cycle (33). Assuming
170 the N-terminal domain of δ remains bound around the β' jaw/N-terminal β' clamp region and the

171 acidic unstructured C-terminal domain is both mobile and flexible, we may propose a mechanism for
172 modulation of transcription (Fig. 2). A closed initiation complex, based on the open complex structure
173 of (9) in which the N-terminal $\sigma_{1.1}$ domain (44) that competes with nucleic acid binding in the primary
174 channel can be modelled *in situ* based on equivalent structures from *E. coli* (24) is shown in Fig. 2A.
175 As the transcription initiation complex transitions from a closed to open complex, the $\sigma_{1.1}$ domain
176 swings out of the primary channel as unwound DNA enters, placing the single stranded template
177 strand with the transcription start site nucleotide located in position for base pairing with the initiating
178 nucleotide triphosphate (9,45).

179

180 Upon $\sigma_{1.1}$ dissociation during formation of the open complex, the δ C-terminal domain would be able
181 to access DNA within the primary channel (Fig. 2B). The highly negative charge of the δ C-terminal
182 domain would encourage dissociation of weakly bound DNA (poor/non-specific promoter sequences
183 bound by σ -factors) (23,36). The cryo EM structure of the *E. coli* RNAP paused EC (PDB ID 6FLP)
184 was used as a template to model termination hairpin RNA in the RNAP_{BS} EC. The model suggests
185 that the highly flexible C-terminal domain of δ is able to interact with both DNA and the RNA
186 transcript in the active site (Fig. 2B and C), consistent with the observation that δ is much more
187 efficient at displacing RNA from an EC than it is DNA (37). In pause/termination complexes the
188 negatively charged δ C-terminal domain would aid the dissociation of RNA facilitating transcription
189 termination and transcription complex recycling (Fig. 2C) (11,36,41).

190

191 ***Comparison of RNAP_{BS} with RNAP from other Firmicutes.***

192

193 *B. subtilis* itself is a biologically and industrially significant organism, being important in soil health
194 and promotion of plant growth, protection from plant pathogens, the industrial production of enzymes
195 (e.g. proteases/amylases), supplements (e.g. nicotinic acid), and antibiotics (e.g. bacitracin), as a
196 probiotic, as a foodstuff (e.g. in natto), and in the study of regulation of gene expression, especially
197 during cellular differentiation in sporulation (2). As the most studied member of the low G+C Gram-
198 positive *Firmicutes* it is also an important model, and closely related to major pathogens including *B.*
199 *cereus*, *B. anthracis*, *Staphylococcus* sp., *Streptococcus* sp., *Enterococcus* sp. and *Clostridium* sp.
200 Organisms such as the *Enterococci* are associated with dissemination of antibiotic resistance
201 determinants, and many clinical isolates of *Staphylococcus* now carry resistance to one or more
202 antibiotics. *S. aureus* is commensal in about 30% of the population and an opportunistic pathogen
203 that remains a major burden on health systems through nosocomial infections, which has been
204 exacerbated in recent years by the rise of community acquired infections (especially methicillin-
205 resistant; MRSA infections) (46). Organisms such as *C. difficile* are associated with diseases difficult

206 to treat successfully with many antibiotics (e.g. *C. difficile* associated diarrhoea (CDAD) relapse is
207 common following vancomycin treatment), and represent a significant burden in terms of both
208 morbidity and mortality to health systems (47). While fidaxomicin was approved by the FDA for
209 treatment of CDAD in 2011, resistance to this drug (lipiarmycin) was first reported in 1977 (48,49),
210 and it is clear new derivatives are needed, as well as a new arsenal of novel compounds to slow the
211 rise of antibiotic resistant infections.

212

213 Sequence alignment of RNAP subunits from representatives of these organisms was performed using
214 *B. subtilis* 168, *S. aureus* USA300, *E. faecalis* V583, *S. pyogenes* M1 GAS, *C. difficile* 630 and *C.*
215 *perfringens* 13 sequences and the resulting CLUSTAL alignment outputs mapped onto the *B. subtilis*
216 elongation complex (PDB ID 6WVJ) in ChimeraX (50,51) with the nucleic acids removed for clarity.
217 The resulting homology sequence maps are shown in Fig. 3 along with a phylogenetic tree produced
218 in MrBayes (52,53) for the *rpoC* (β' subunit) using the *E. coli rpoC* sequence as an outlier to root the
219 tree. The bootstrap probability values of 1 indicate absolute confidence in the branch divisions and
220 lengths, and agree perfectly, as expected, with the segregation of *B. subtilis* and *S. aureus* to the
221 *Bacilli*, *S. pyogenes* and *E. faecalis* to the *Lactobacilli*, and *C. difficile* and *C. perfringens* to the
222 *Clostridia*.

223

224 The level of sequence conservation is high, especially in the β and β' clamps, active site and β flap
225 where the majority of the functional motifs (see Fig. 1C and D) are found. Although the β ln5 is
226 present in all of the organism from which sequences were selected, the level of sequence conservation
227 is relatively low in the major β lobe and β ln5 region (Fig. 3C), consistent with the hypothesis (above)
228 that this region maybe important for providing class/order/species-specific binding sites for
229 transcription factors. *B. subtilis*-specific sequences that are absent in the other organisms, such as the
230 10 amino acid insert at β E696-G705 that protrudes from the bottom of the structure are shown in
231 yellow (Fig. 3B and C). Given the industrial and medical importance of this group of bacteria, regions
232 of identity/difference can be targeted in functional studies or exploited in the rational design of
233 inhibitor compounds as new antimicrobial leads.

234

235 ***Antimicrobial development options***

236 Transcription is an underutilised target for new antibiotic development, although significant efforts
237 are currently underway to identify promising new leads and to improve the properties of existing
238 clinical compounds (48,54). Many promising compounds fail to make it to market as broad spectrum
239 antibiotics due to the problems of identifying hits that are able to cross the outer membrane of Gram
240 negative bacteria, despite showing excellent activity against Gram positives. Infections due to the

241 *Firmicutes*, including *S. aureus*, *C. difficile*, vancomycin-resistant *Enterococcus*, and drug resistant
242 *Streptococcus* (Group A and B), have been identified by the Centre for Disease Control (CDC) as
243 organisms of major clinical concern for which new approaches/treatments for infection are required
244 (47), and there is a case for developing more narrow spectrum drugs that target this group.
245 Nevertheless, significant hurdles still remain that must be dealt with (55).

246

247 Fidaxomicin is a semi-synthetic macrolide that inhibits transcription initiation and was approved for
248 use in CDAD in 2012. *C. difficile* (and other *Clostridia*) are exquisitely sensitive to fidaxomicin, but
249 this is not a property shared by most other *Firmicutes* with some *Streptococci* being $> 500 \times$ more
250 resistant than *C. difficile* (56). Structures of fidaxomicin in complex with RNAP from *Mycobacterium*
251 *tuberculosis* have been solved (57,58) enabling modelling of the drug bound to the *B. subtilis*
252 holoenzyme (PDB ID 7CKQ) with sequence alignments to pathogenic *Firmicutes* homology mapped
253 as in the previous section (Fig. 4A). Other than the homodichloro-orsellenyl moiety that is adjacent
254 to the β -flap tip and -35 promoter sequence binding σ region 4, the bulk of fidaxomicin is buried
255 within the enzyme at the base of the RNAP clamp. All of the RNAP and σ sequences the remaining
256 bulk of fidaxomicin interacts with (switch regions Sw2, Sw3, Sw4 and the σ finger; (57,58)) are
257 highly conserved (pink, Fig. 4A, right side box) consistent with the broad spectrum activity of this
258 compound in *in vitro* transcription assays (although *E. coli* holoenzyme is quite resistant to
259 fidaxomicin; (57)). Increasing the spectrum of activity of fidaxomicin may depend on improving cell
260 permeability properties, especially for organisms such a *S. pneumoniae*, where production of a
261 capsule layer may inhibit efficient cell penetration.

262

263 An area of antimicrobial research that is showing promise for compounds highly active against
264 *Firmicutes* is the development of compounds that inhibit the essential interaction between RNAP and
265 σ^A . Establishment of a functional holoenzyme complex is dependent on the interaction between a
266 small region of the $\sigma_{2.2}$ region with the β' clamp helix (CH) (59,60). These sequences are highly
267 conserved in the *Firmicutes* (Fig. 4B), and across the eubacteria, making this an excellent target for
268 the development of molecules that inhibit this essential protein-protein interaction (PPI) (48,61).
269 Multiple research programs involving high-throughput small molecule screens, structure-based drug
270 design, and small peptide antagonists have yielded promising results (62-71). PPIs are an attractive
271 target for drug development as simultaneous complementary mutations are required at two unlinked
272 genetic loci to confer resistance to a compound whilst retaining the interaction, which has the
273 potential to substantially reduce the rate at which resistance develops (72).

274

275 Mutagenesis studies to quantify the importance of specific amino acid residues in formation of
276 holoenzyme have been determined (Fig. 4B right, (59)) that have enabled the construction of
277 pharmacophores for screening compound libraries for potential inhibitor molecules. A major issue
278 with such a target is that the interaction site between $\sigma_{2.2}$ and the β' clamp helix is relatively flat
279 making binding specificity and avidity potentially problematic. Nevertheless, compounds have been
280 developed that are highly specific for bacterial initiation complexes, showing no binding activity
281 against human RNAP, and that target initiation complex formation in live bacterial cells as
282 determined by cytological assay (65). Whilst many of these compounds show limited or no activity
283 against Gram negative bacteria, excellent results have been obtained against Gram positive bacteria,
284 including those carrying resistance to multiple antibiotics providing an avenue for development of
285 new drugs effective against Gram positive pathogens (65,66,69,70).

286

287 ***Concluding statement***

288

289 Determination of the structure of RNAP from *B. subtilis* now opens the way to undertake detailed
290 structure-function studies on the mechanism of transcription in this Gram-positive model, particularly
291 with respect to mechanistic aspects that are different to *E. coli* helping provide a more holistic
292 understanding of the mechanism of microbial transcription. In addition, this structural information
293 will be important in providing a platform for the rational design and subsequent development of new
294 lead antibiotics to combat infections caused by the *Firmicutes*.

295

296

297 ***Acknowledgments***

298 This work was supported by funding from the Australian Research Council (DP210100365) to PJL
299 and AJO. MM was supported by a PhD scholarship from the University of Newcastle Priority
300 Research Centre for Drug Discovery.

301

302

303

304 **References**

- 305
- 306 1. Browning, D.F. and Busby, S.J. (2016) Local and global regulation of transcription initiation
307 in bacteria. *Nat Rev Microbiol*, **14**, 638-650.
- 308 2. Errington, J. and Aart, L.T.V. (2020) Microbe Profile: *Bacillus subtilis*: model organism for
309 cellular development, and industrial workhorse. *Microbiology (Reading)*, **166**, 425-427.
- 310 3. Benjin, X. and Ling, L. (2020) Developments, applications, and prospects of cryo-electron
311 microscopy. *Protein Sci*, **29**, 872-882.
- 312 4. Chen, J., Wassarman, K.M., Feng, S., Leon, K., Feklistov, A., Winkelman, J.T., Li, Z., Walz, T.,
313 Campbell, E.A. and Darst, S.A. (2017) 6S RNA Mimics B-Form DNA to Regulate *Escherichia*
314 *coli* RNA Polymerase. *Mol Cell*, **68**, 388-397 e386.
- 315 5. Guo, X., Myasnikov, A.G., Chen, J., Crucifix, C., Papai, G., Takacs, M., Schultz, P. and
316 Weixlbaumer, A. (2018) Structural Basis for NusA Stabilized Transcriptional Pausing. *Mol*
317 *Cell*, **69**, 816-827 e814.
- 318 6. Abdelkareem, M., Saint-Andre, C., Takacs, M., Papai, G., Crucifix, C., Guo, X., Ortiz, J. and
319 Weixlbaumer, A. (2019) Structural Basis of Transcription: RNA Polymerase Backtracking
320 and Its Reactivation. *Mol Cell*, **75**, 298-309 e294.
- 321 7. Kang, J.Y., Llewellyn, E., Chen, J., Olinares, P.D.B., Brewer, J., Chait, B.T., Campbell, E.A. and
322 Darst, S.A. (2021) Structural basis for transcription complex disruption by the Mfd
323 translocase. *Elife*, **10**.
- 324 8. Said, N., Hilal, T., Sunday, N.D., Khatri, A., Burger, J., Mielke, T., Belogurov, G.A., Loll, B.,
325 Sen, R., Artsimovitch, I. *et al.* (2021) Steps toward translocation-independent RNA
326 polymerase inactivation by terminator ATPase rho. *Science*, **371**.
- 327 9. Fang, C., Li, L., Zhao, Y., Wu, X., Philips, S.J., You, L., Zhong, M., Shi, X., O'Halloran, T.V., Li,
328 Q. *et al.* (2020) The bacterial multidrug resistance regulator BmrR distorts promoter DNA
329 to activate transcription. *Nat Commun*, **11**, 6284.
- 330 10. Newing, T.P., Oakley, A.J., Miller, M., Dawson, C.J., Brown, S.H.J., Bouwer, J.C., Tolun, G.
331 and Lewis, P.J. (2020) Molecular basis for RNA polymerase-dependent transcription
332 complex recycling by the helicase-like motor protein Held. *Nat Commun*, **11**, 6420.
- 333 11. Pei, H.H., Hilal, T., Chen, Z.A., Huang, Y.H., Gao, Y., Said, N., Loll, B., Rappaport, J.,
334 Belogurov, G.A., Artsimovitch, I. *et al.* (2020) The delta subunit and NTPase Held institute a
335 two-pronged mechanism for RNA polymerase recycling. *Nat Commun*, **11**, 6418.
- 336 12. Ishikawa, S., Oshima, T., Kurokawa, K., Kusuya, Y. and Ogasawara, N. (2010) RNA
337 polymerase trafficking in *Bacillus subtilis* cells. *J Bacteriol*, **192**, 5778-5787.
- 338 13. Mooney, R.A., Davis, S.E., Peters, J.M., Rowland, J.L., Ansari, A.Z. and Landick, R. (2009)
339 Regulator trafficking on bacterial transcription units in vivo. *Mol Cell*, **33**, 97-108.
- 340 14. Krasny, L. and Gourse, R.L. (2004) An alternative strategy for bacterial ribosome synthesis:
341 *Bacillus subtilis* rRNA transcription regulation. *EMBO J*, **23**, 4473-4483.
- 342 15. Ma, C., Mobli, M., Yang, X., Keller, A.N., King, G.F. and Lewis, P.J. (2015) RNA polymerase-
343 induced remodelling of NusA produces a pause enhancement complex. *Nucleic Acids Res*,
344 **43**, 2829-2840.
- 345 16. Newberry, K.J., Nakano, S., Zuber, P. and Brennan, R.G. (2005) Crystal structure of the
346 *Bacillus subtilis* anti-alpha, global transcriptional regulator, Spx, in complex with the alpha
347 C-terminal domain of RNA polymerase. *Proc Natl Acad Sci U S A*, **102**, 15839-15844.
- 348 17. Hudson, B.P., Quispe, J., Lara-Gonzalez, S., Kim, Y., Berman, H.M., Arnold, E., Ebright, R.H.
349 and Lawson, C.L. (2009) Three-dimensional EM structure of an intact activator-dependent
350 transcription initiation complex. *Proc Natl Acad Sci U S A*, **106**, 19830-19835.

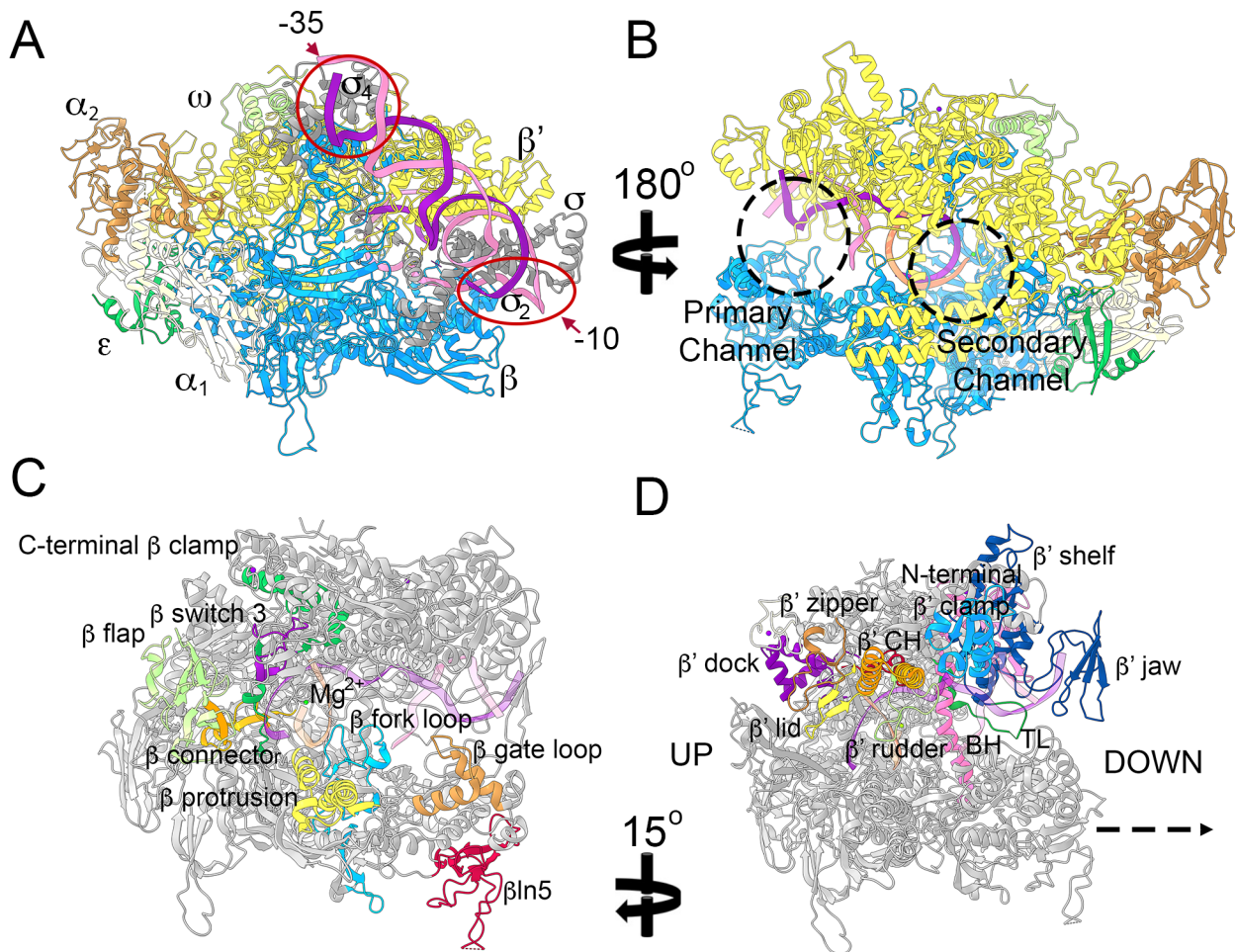
- 351 18. Krupp, F., Said, N., Huang, Y.H., Loll, B., Burger, J., Mielke, T., Spahn, C.M.T. and Wahl, M.C.
352 (2019) Structural Basis for the Action of an All-Purpose Transcription Anti-termination
353 Factor. *Mol Cell*, **74**, 143-157 e145.
- 354 19. Ghosh, P., Ishihama, A. and Chatterji, D. (2001) Escherichia coli RNA polymerase subunit
355 omega and its N-terminal domain bind full-length beta' to facilitate incorporation into the
356 alpha2beta subassembly. *Eur J Biochem*, **268**, 4621-4627.
- 357 20. Minakhin, L., Bhagat, S., Brunning, A., Campbell, E.A., Darst, S.A., Ebright, R.H. and
358 Severinov, K. (2001) Bacterial RNA polymerase subunit omega and eukaryotic RNA
359 polymerase subunit RPB6 are sequence, structural, and functional homologs and promote
360 RNA polymerase assembly. *Proc Natl Acad Sci U S A*, **98**, 892-897.
- 361 21. Keller, A.N., Yang, X., Wiedermannova, J., Delumeau, O., Krasny, L. and Lewis, P.J. (2014)
362 epsilon, a new subunit of RNA polymerase found in gram-positive bacteria. *J Bacteriol*, **196**,
363 3622-3632.
- 364 22. Spiegelman, G.B., Hiatt, W.R. and Whiteley, H.R. (1978) Role of the 21,000 molecular
365 weight polypeptide of *Bacillus subtilis* RNA polymerase in RNA synthesis. *J Biol Chem*, **253**,
366 1756-1765.
- 367 23. Weiss, A. and Shaw, L.N. (2015) Small things considered: the small accessory subunits of
368 RNA polymerase in Gram-positive bacteria. *FEMS Microbiol Rev*, **39**, 541-554.
- 369 24. Bae, B., Davis, E., Brown, D., Campbell, E.A., Wigneshweraraj, S. and Darst, S.A. (2013)
370 Phage T7 Gp2 inhibition of Escherichia coli RNA polymerase involves misappropriation of
371 sigma70 domain 1.1. *Proc Natl Acad Sci U S A*, **110**, 19772-19777.
- 372 25. Lane, W.J. and Darst, S.A. (2010) Molecular evolution of multisubunit RNA polymerases:
373 structural analysis. *J Mol Biol*, **395**, 686-704.
- 374 26. Lane, W.J. and Darst, S.A. (2010) Molecular evolution of multisubunit RNA polymerases:
375 sequence analysis. *J Mol Biol*, **395**, 671-685.
- 376 27. Wang, C., Molodtsov, V., Firlar, E., Kaelber, J.T., Blaha, G., Su, M. and Ebright, R.H. (2020)
377 Structural basis of transcription-translation coupling. *Science*, **369**, 1359-1365.
- 378 28. Harriott, K. (2012), The University of Newcastle.
- 379 29. Sanders, K., Lin, C.L., Smith, A.J., Cronin, N., Fisher, G., Eftychidis, V., McGlynn, P., Savery,
380 N.J., Wigley, D.B. and Dillingham, M.S. (2017) The structure and function of an RNA
381 polymerase interaction domain in the PcrA/UvrD helicase. *Nucleic Acids Res*, **45**, 3875-
382 3887.
- 383 30. Delumeau, O., Lecointe, F., Muntel, J., Guillot, A., Guedon, E., Monnet, V., Hecker, M.,
384 Becher, D., Polard, P. and Noirot, P. (2011) The dynamic protein partnership of RNA
385 polymerase in *Bacillus subtilis*. *Proteomics*, **11**, 2992-3001.
- 386 31. Gwynn, E.J., Smith, A.J., Guy, C.P., Savery, N.J., McGlynn, P. and Dillingham, M.S. (2013) The
387 conserved C-terminus of the PcrA/UvrD helicase interacts directly with RNA polymerase.
388 *PLoS One*, **8**, e78141.
- 389 32. Noirot-Gros, M.F., Dervyn, E., Wu, L.J., Mervelet, P., Errington, J., Ehrlich, S.D. and Noirot,
390 P. (2002) An expanded view of bacterial DNA replication. *Proc Natl Acad Sci U S A*, **99**,
391 8342-8347.
- 392 33. Doherty, G.P., Fogg, M.J., Wilkinson, A.J. and Lewis, P.J. (2010) Small subunits of RNA
393 polymerase: localization, levels and implications for core enzyme composition.
394 *Microbiology*, **156**, 3532-3543.
- 395 34. Kuban, V., Srb, P., Stegnerova, H., Padra, P., Zachrdla, M., Jasenakova, Z., Sanderova, H.,
396 Vitovska, D., Krasny, L., Koval, T. *et al.* (2019) Quantitative Conformational Analysis of
397 Functionally Important Electrostatic Interactions in the Intrinsically Disordered Region of
398 Delta Subunit of Bacterial RNA Polymerase. *J Am Chem Soc*, **141**, 16817-16828.

- 399 35. Motackova, V., Sanderova, H., Zidek, L., Novacek, J., Padrta, P., Svenkova, A., Korelusova, J.,
400 Jonak, J., Krasny, L. and Sklenar, V. (2010) Solution structure of the N-terminal domain of
401 *Bacillus subtilis* delta subunit of RNA polymerase and its classification based on structural
402 homologs. *Proteins*, **78**, 1807-1810.
- 403 36. Juang, Y.L. and Helmann, J.D. (1994) The delta subunit of *Bacillus subtilis* RNA polymerase.
404 An allosteric effector of the initiation and core-recycling phases of transcription. *J Mol Biol*,
405 **239**, 1-14.
- 406 37. Lopez de Saro, F.J., Woody, A.Y. and Helmann, J.D. (1995) Structural analysis of the *Bacillus*
407 *subtilis* delta factor: a protein polyanion which displaces RNA from RNA polymerase. *J Mol Biol*,
408 **252**, 189-202.
- 409 38. Lopez de Saro, F.J., Yoshikawa, N. and Helmann, J.D. (1999) Expression, abundance, and
410 RNA polymerase binding properties of the delta factor of *Bacillus subtilis*. *J Biol Chem*, **274**,
411 15953-15958.
- 412 39. Nicolas, P., Mader, U., Dervyn, E., Rochat, T., Leduc, A., Pigeonneau, N., Bidnenko, E.,
413 Marchadier, E., Hoebelke, M., Aymerich, S. *et al.* (2012) Condition-dependent
414 transcriptome reveals high-level regulatory architecture in *Bacillus subtilis*. *Science*, **335**,
415 1103-1106.
- 416 40. Rabatinova, A., Sanderova, H., Jirat Matejckova, J., Korelusova, J., Sojka, L., Barvik, I.,
417 Papouskova, V., Sklenar, V., Zidek, L. and Krasny, L. (2013) The delta subunit of RNA
418 polymerase is required for rapid changes in gene expression and competitive fitness of the
419 cell. *J Bacteriol*, **195**, 2603-2611.
- 420 41. Wiedermannova, J., Sudzinova, P., Koval, T., Rabatinova, A., Sanderova, H., Ramanuk, O.,
421 Rittich, S., Dohnalek, J., Fu, Z., Halada, P. *et al.* (2014) Characterization of Held, an
422 interacting partner of RNA polymerase from *Bacillus subtilis*. *Nucleic Acids Res*, **42**, 5151-
423 5163.
- 424 42. Prajapati, R.K., Sengupta, S., Rudra, P. and Mukhopadhyay, J. (2016) *Bacillus subtilis* delta
425 Factor Functions as a Transcriptional Regulator by Facilitating the Open Complex
426 Formation. *J Biol Chem*, **291**, 1064-1075.
- 427 43. de Jong, L., de Koning, E.A., Roseboom, W., Buncherd, H., Wanner, M.J., Dapic, I., Jansen,
428 P.J., van Maarseveen, J.H., Corthals, G.L., Lewis, P.J. *et al.* (2017) In-Culture Cross-Linking of
429 Bacterial Cells Reveals Large-Scale Dynamic Protein-Protein Interactions at the Peptide
430 Level. *J Proteome Res*, **16**, 2457-2471.
- 431 44. Zachrdla, M., Padrta, P., Rabatinova, A., Sanderova, H., Barvik, I., Krasny, L. and Zidek, L.
432 (2017) Solution structure of domain 1.1 of the sigma(A) factor from *Bacillus subtilis* is
433 preformed for binding to the RNA polymerase core. *J Biol Chem*, **292**, 11610-11617.
- 434 45. Murakami, K.S. and Darst, S.A. (2003) Bacterial RNA polymerases: the wholo story. *Curr
435 Opin Struct Biol*, **13**, 31-39.
- 436 46. Tong, S.Y., Davis, J.S., Eichenberger, E., Holland, T.L. and Fowler, V.G., Jr. (2015)
437 *Staphylococcus aureus* infections: epidemiology, pathophysiology, clinical manifestations,
438 and management. *Clin Microbiol Rev*, **28**, 603-661.
- 439 47. CDC. (2013), *Centre for Disease Control*.
- 440 48. Ma, C., Yang, X. and Lewis, P.J. (2016) Bacterial Transcription as a Target for Antibacterial
441 Drug Development. *Microbiol Mol Biol Rev*, **80**, 139-160.
- 442 49. Sonenshein, A.L., Alexander, H.B., Rothstein, D.M. and Fisher, S.H. (1977) Lipiarmycin-
443 resistant ribonucleic acid polymerase mutants of *Bacillus subtilis*. *J Bacteriol*, **132**, 73-79.
- 444 50. Goddard, T.D., Huang, C.C., Meng, E.C., Pettersen, E.F., Couch, G.S., Morris, J.H. and Ferrin,
445 T.E. (2018) UCSF ChimeraX: Meeting modern challenges in visualization and analysis.
446 *Protein Sci*, **27**, 14-25.

- 447 51. Pettersen, E.F., Goddard, T.D., Huang, C.C., Meng, E.C., Couch, G.S., Croll, T.I., Morris, J.H.
448 and Ferrin, T.E. (2020) UCSF ChimeraX: Structure Visualization for Researchers, Educators,
449 and Developers. *Protein Sci.*
- 450 52. Huelsenbeck, J.P. and Ronquist, F. (2001) MRBAYES: Bayesian inference of phylogenetic
451 trees. *Bioinformatics*, **17**, 754-755.
- 452 53. Ronquist, F., Teslenko, M., van der Mark, P., Ayres, D.L., Darling, A., Hohna, S., Larget, B.,
453 Liu, L., Suchard, M.A. and Huelsenbeck, J.P. (2012) MrBayes 3.2: efficient Bayesian
454 phylogenetic inference and model choice across a large model space. *Syst Biol*, **61**, 539-
455 542.
- 456 54. Maffioli, S.I., Zhang, Y., Degen, D., Carzaniga, T., Del Gatto, G., Serina, S., Monciardini, P.,
457 Mazzetti, C., Guglierame, P., Candiani, G. *et al.* (2017) Antibacterial Nucleoside-Analog
458 Inhibitor of Bacterial RNA Polymerase. *Cell*, **169**, 1240-1248 e1223.
- 459 55. Alm, R.A. and Lahiri, S.D. (2020) Narrow-Spectrum Antibacterial Agents-Benefits and
460 Challenges. *Antibiotics (Basel)*, **9**.
- 461 56. Goldstein, E.J., Babakhani, F. and Citron, D.M. (2012) Antimicrobial activities of fidaxomicin.
462 *Clin Infect Dis*, **55 Suppl 2**, S143-148.
- 463 57. Boyaci, H., Chen, J., Lilic, M., Palka, M., Mooney, R.A., Landick, R., Darst, S.A. and Campbell,
464 E.A. (2018) Fidaxomicin jams Mycobacterium tuberculosis RNA polymerase motions
465 needed for initiation via RbpA contacts. *Elife*, **7**.
- 466 58. Lin, W., Das, K., Degen, D., Mazumder, A., Duchi, D., Wang, D., Ebright, Y.W., Ebright, R.Y.,
467 Sineva, E., Gigliotti, M. *et al.* (2018) Structural Basis of Transcription Inhibition by
468 Fidaxomicin (Liparmycin A3). *Mol Cell*, **70**, 60-71 e15.
- 469 59. Johnston, E.B., Lewis, P.J. and Griffith, R. (2009) The interaction of *Bacillus subtilis* sigmaA
470 with RNA polymerase. *Protein Sci*, **18**, 2287-2297.
- 471 60. Arthur, T.M., Anthony, L.C. and Burgess, R.R. (2000) Mutational analysis of beta '260-309, a
472 sigma 70 binding site located on *Escherichia coli* core RNA polymerase. *J Biol Chem*, **275**,
473 23113-23119.
- 474 61. Cossar, P.J., Lewis, P.J. and McCluskey, A. (2020) Protein-protein interactions as antibiotic
475 targets: A medicinal chemistry perspective. *Med Res Rev*, **40**, 469-494.
- 476 62. Andre, E., Bastide, L., Michaux-Charachon, S., Gouby, A., Villain-Guillot, P., Latouche, J.,
477 Bouchet, A., Gaultier, M. and Leonetti, J.P. (2006) Novel synthetic molecules targeting the
478 bacterial RNA polymerase assembly. *J Antimicrob Chemother*, **57**, 245-251.
- 479 63. Glaser, B.T., Bergendahl, V., Thompson, N.E., Olson, B. and Burgess, R.R. (2007) LRET-based
480 HTS of a small-compound library for inhibitors of bacterial RNA polymerase. *Assay Drug
481 Dev Technol*, **5**, 759-768.
- 482 64. Husecken, K., Negri, M., Fruth, M., Boettcher, S., Hartmann, R.W. and Haupenthal, J. (2013)
483 Peptide-Based Investigation of the *Escherichia coli* RNA Polymerase sigma(70):Core
484 Interface As Target Site. *ACS Chem Biol*.
- 485 65. Ma, C., Yang, X. and Lewis, P.J. (2016) Bacterial Transcription Inhibitor of RNA Polymerase
486 Holoenzyme Formation by Structure-Based Drug Design: From in Silico Screening to
487 Validation. *ACS Infect Dis*, **2**, 39-46.
- 488 66. Ma, C., Yang, X., Kandemir, H., Mielczarek, M., Johnston, E.B., Griffith, R., Kumar, N. and
489 Lewis, P.J. (2013) Inhibitors of bacterial transcription initiation complex formation. *ACS
490 Chem Biol*, **8**, 1972-1980.
- 491 67. Mielczarek, M., Thomas, R.V., Ma, C., Kandemir, H., Yang, X., Bhadbhade, M., Black, D.S.,
492 Griffith, R., Lewis, P.J. and Kumar, N. (2015) Synthesis and biological activity of novel mono-
493 indole and mono-benzofuran inhibitors of bacterial transcription initiation complex
494 formation. *Bioorg Med Chem*, **23**, 1763-1775.

- 495 68. Wenholz, D.S., Zeng, M., Ma, C., Mielczarek, M., Yang, X., Bhadbhade, M., Black, D.S.C.,
496 Lewis, P.J., Griffith, R. and Kumar, N. (2017) Small molecule inhibitors of bacterial
497 transcription complex formation. *Bioorg Med Chem Lett*, **27**, 4302-4308.
- 498 69. Ye, J., Chu, A.J., Harper, R., Chan, S.T., Shek, T.L., Zhang, Y., Ip, M., Sambir, M., Artsimovitch,
499 I., Zuo, Z. *et al.* (2020) Discovery of Antibacterials That Inhibit Bacterial RNA Polymerase
500 Interactions with Sigma Factors. *J Med Chem*, **63**, 7695-7720.
- 501 70. Ye, J., Chu, A.J., Lin, L., Chan, S.T., Harper, R., Xiao, M., Artsimovitch, I., Zuo, Z., Ma, C. and
502 Yang, X. (2020) Benzyl and benzoyl benzoic acid inhibitors of bacterial RNA polymerase-
503 sigma factor interaction. *Eur J Med Chem*, **208**, 112671.
- 504 71. Sartini, S., Levati, E., Maccesi, M., Guerra, M., Spadoni, G., Bach, S., Benincasa, M., Scocchi,
505 M., Ottonello, S., Rivara, S. *et al.* (2019) New Antimicrobials Targeting Bacterial RNA
506 Polymerase Holoenzyme Assembly Identified with an in Vivo BRET-Based Discovery
507 Platform. *ACS Chem Biol*, **14**, 1727-1736.
- 508 72. Igler, C., Rolff, J. and Regoes, R. (2021) Multi-step vs. single-step resistance evolution under
509 different drugs, pharmacokinetics and treatment regimens. *Elife*, **10**.
- 510

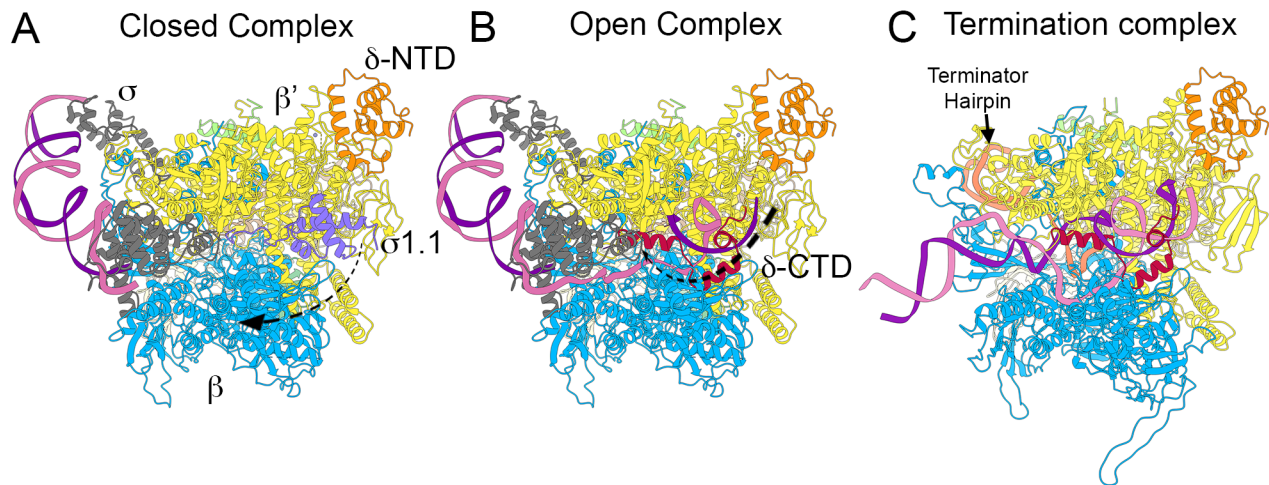
511 **Figures**



512

513 **Figure 1. Structure of *B. subtilis* RNAP.** Panel A shows the structure of RNAP holoenzyme, and
514 Panel B an elongation complex. Subunit colouring; α_1 cream, α_2 brown, β blue, β' yellow, ε dark
515 green, ω pale green, σ grey. Template strand DNA is shown in dark purple, non-template strand DNA
516 in pink, and RNA in orange. The -10 and -35 promoter elements are ringed in Panel A, and the
517 primary and secondary channels circled in Panel B. Panels C and D show key functional elements of
518 the β and β' subunits, respectively, as defined by (11). β subunit elements in Panel B; C-terminal β
519 clamp dark green, β switch 3 purple, β flap pale green, β connector vermillion, β protrusion yellow,
520 β fork loop blue, β gate loop orange, $\beta\text{ln}5$ red. β' subunit elements in Panel C; β' dock purple, β' lid
521 yellow, β' zipper orange and clamp helix (CH) orange, β' rudder pale green, β' clamp blue, β' shelf
522 and jaw dark blue, bridge helix (BH) pink, trigger loop (TL) dark green. Up, and downstream sides
523 of RNAP are indicated for reference.

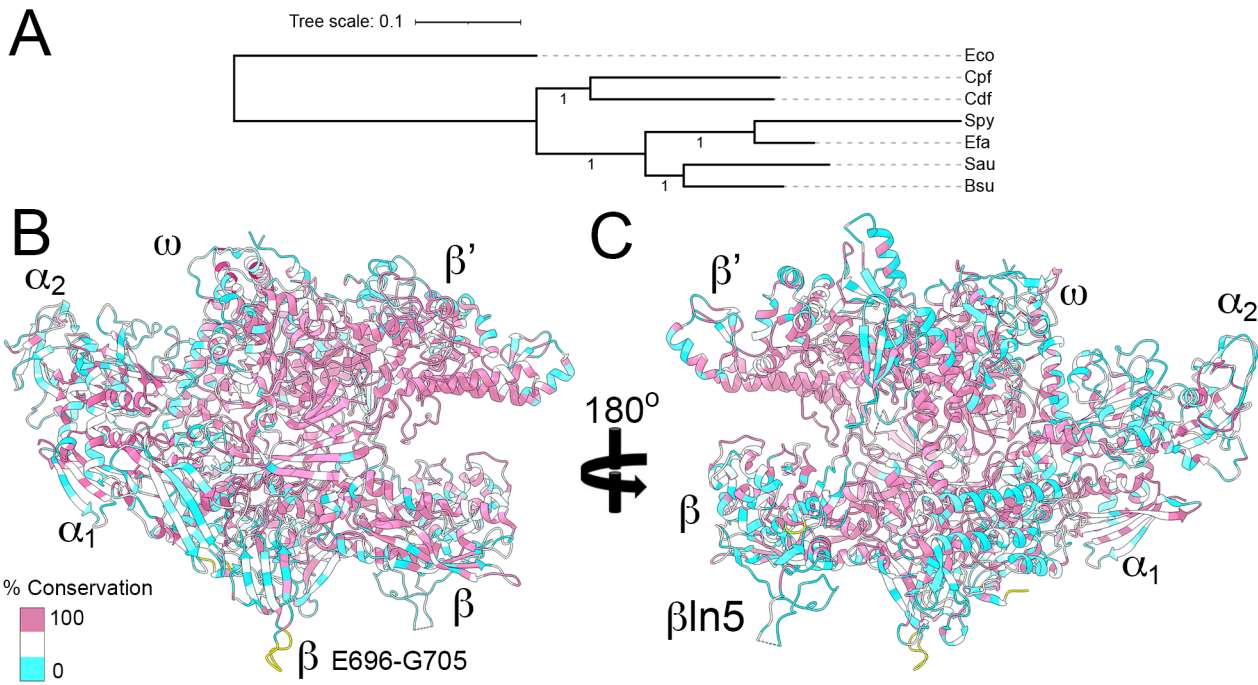
524



525

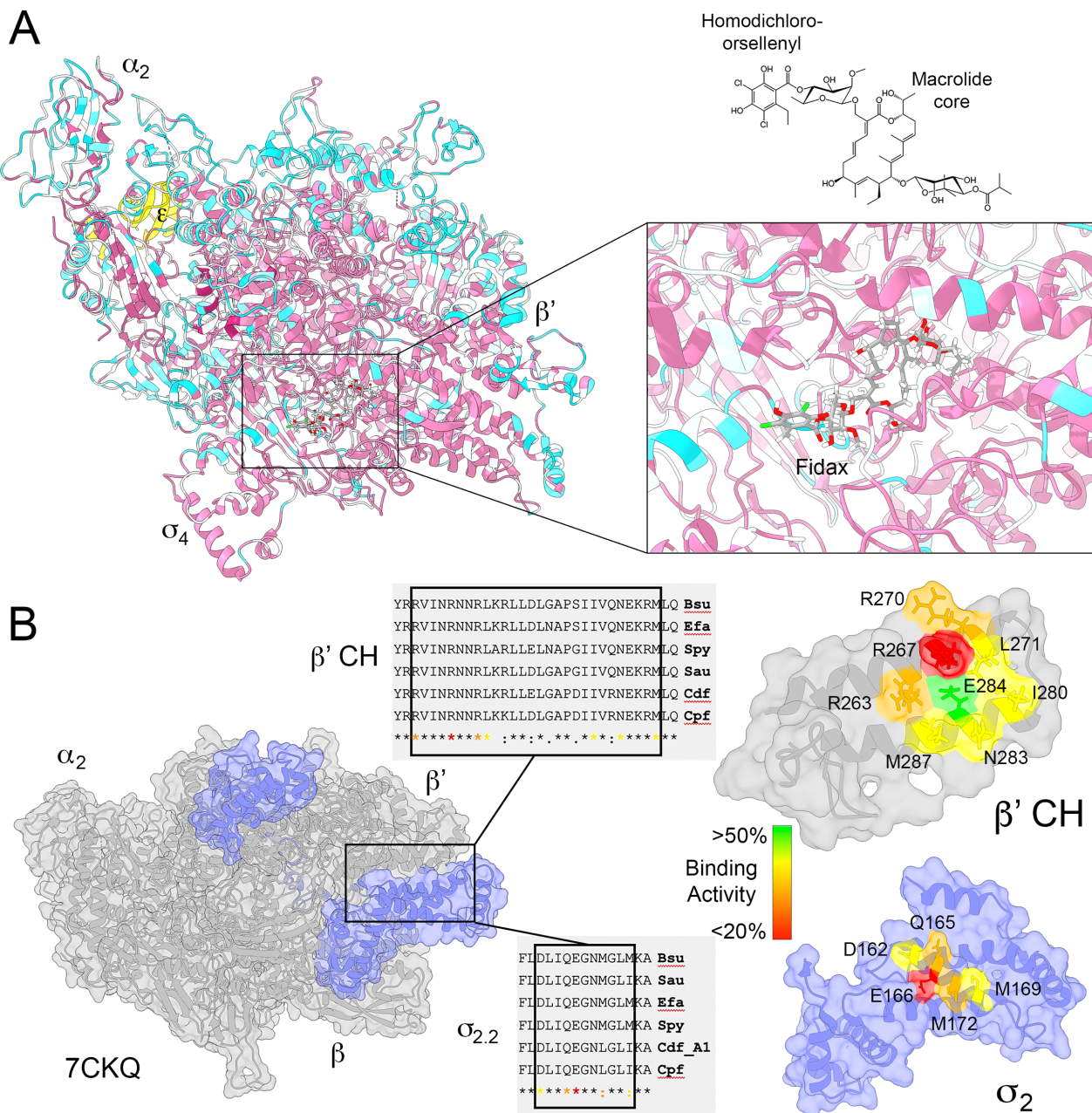
526 **Figure 2. A model for δ subunit activity during transcription initiation and termination.** In all
527 panels RNAP subunits are coloured as in Figure 1 with the addition of σ region 1.1 (σ1.1) shown in
528 lavender, the N-terminal domain of δ (δ-NTD) in orange, and the C-terminal domain (δ-CTD) in red.
529 Panel A shows a closed transcription initiation complex with the δ-NTD bound around the β' shelf.
530 The CTD is not shown (see text for details). σ1.1 is shown in primary channel with the arrow
531 indicating the dissociation of σ1.1 from this site during the transition from a closed to open initiation
532 complex. Panel B shows an open complex in which promoter DNA strands have separated and the
533 template strand has moved into the active site within the primary channel. δ-CTD is shown moving
534 into the primary channel where, due to its polyanionic nature it is able to compete with DNA in the
535 primary channel helping to prevent transcription initiation from cryptic/weak promoters. Panel C
536 shows a model of a transcription termination complex with a RNA hairpin (terminator hairpin). . in
537 the RNA exit channel. The polyanionic δ-CTD is able to disrupt the RNA-DNA hybrid upstream
538 from the active site aiding dissociation of RNA from the complex and RNAP recycling following
539 termination of transcription.

540



542 **Figure 3. Mapping sequence conservation of pathogenic *Firmicutes* to *B. subtilis* RNAP.** Panel
543 A shows a Bayesian tree of sequence alignments of the β subunit of *B. subtilis* (Bsu), *S. aureus*
544 (Sau), *E. faecalis* (Efa), *S. pyogenes* (Spy), *C. difficile* (Cdf), and *C. perfringens* (Cpf). The
545 sequence of *E. coli* β subunit (Eco) was used to root the tree. Tree scale represents amino acid
546 substitutions per site. Bootstrap values are shown on the branches. Panels B and C show up- and
547 downstream views of RNAP, respectively. Subunits are labelled as well as the common to
548 *Firmicutes* β ln5 insert, and *B. subtilis*-specific β E696-G705 insert (yellow). A colour scale for
549 sequence conservation shown on the structures is shown on the bottom left of Panel B with
550 sequences 100% conserved pink, 0% conserved cyan and >0, <100 in white.

551



552

553 **Figure 4. Transcription inhibition drug targets in *Firmicutes* RNAP.** Panel A shows sequence
 554 conservation mapping of pathogenic *Firmicutes* with colouring as in Figure 3 mapped onto the *B.*
 555 *subtilis* RNAP holoenzyme. The α_2 , and β' subunits and σ_4 domain are labelled for reference. The ϵ
 556 subunit which is not conserved in *Clostridia* is shown in yellow. Fidaxomicin (Fidax) is shown
 557 docked in the holoenzyme structure (box), which is shown in an enlarged box on the right (see text
 558 for details). The structure of fidaxomicin is shown above the right hand box approximately aligned
 559 for reference with the homodichloro-orsellenny and macrolide core labelled for reference. Panel B,
 560 left, shows *B. subtilis* holoenzyme with core subunits coloured grey and σ^A in pale blue. The box
 561 indicates the interaction site between the β' CH and $\sigma_{2.2}$ regions essential for formation of
 562 holoenzyme. Sequence alignments of the relevant regions are shown adjacent to the holoenzyme.
 563 Note, *C. difficile* encodes two σ^A subunits, but only the alignment for *sigA1* is shown as *sigA2* is not

564 expressed to a significant level during vegetative growth. Strain labelling is the same as in Figure 3.
565 The right hand side shows enlarged regions of the β' CH and $\sigma_{2.2}$ regions with amino acids involved
566 in formation of the holoenzyme colour coded according to their importance as determined from
567 mutagenesis studies (59). The colour ramp indicates the relative binding activity mutation causes to
568 holoenzyme formation.